

# Wind Energy Conversion System for Harmonics and Inter-harmonic Analysis

Emmanuel Hernández<sup>a\*</sup>, Miguel Ángel Hernández<sup>b</sup>, Hugo Jorge Cortina Marrero<sup>c</sup>, Reynaldo Iracheta<sup>d</sup>

<sup>a,b</sup>Universidad del Istmo, Calle Sta. Cruz s/n Av. Universidad, Oaxaca. C.P. 70760, México

<sup>a</sup>Email: emanuel.mayoral7@gmail.com; <sup>b</sup>Email: mahluni2000@yahoo.com.mx

<sup>c</sup>Email: hcmlhd@yahoo.com; <sup>d</sup>Email: riracheta@conacyt.mx

## Abstract

In this research, a harmonic and inter-harmonic analysis is presented for two types of wind energy conversion systems (WECS): a squirrel cage induction machine and doubly-fed induction machine because of the incorporation of power electronics in these systems, such as soft-starter and power converter that distort the voltage and current waveform. The analysis is based on the well-known steady-state induction machine model, additionally; a dynamic-state model is developed to compare the steady-state model validating the results of the simulations obtaining a harmonic and inter-harmonic model, in steady-state, clear and precise of the wind energy conversion system.

**Keywords:** Doubly-fed induction machine; harmonic and inter-harmonic analysis; wind energy conversion system.

## 1. Introduction

The increase in power generated in wind farms makes it necessary to study the power quality injected into the electrical network, transmission systems and electrical machinery. This power generated can present problems mainly due to three factors:

1. Introduction of voltage fluctuations and the presence of harmonics and inter-harmonic in the electrical network due to natural oscillations in wind velocity, and those caused by the presence of the mast.

---

\* Corresponding author.

2. Stability problems of the wind turbines due to contingencies in the electrical network (short-circuits, lightning, maneuvers, etc.), as well as those due to the great variability of the wind.
3. Problems of prediction and planning in power generated.

Currently, one of the problems that has the wind turbine connected to the electrical networks is the intermittence of the injected power to network by the wind dependence and, on the other hand, the injection of harmonic currents to the electrical network due to the use of power electronics for their connection.

The type of technology of wind turbines conversion system used in wind farms determines the power quality. For example, the fixed-velocity wind turbines based in squirrel cage induction machine, the element that causes distortion of the current is the soft-starter, formed by a thyristors bridge, which not in all operations of the turbine is in operation. On the other hand, variable-velocity wind turbines today have in common the use of electronic power converters to be able to vary the velocity and to maintain the power factor within the desired limits. This is done with a switching control that applies a pulse width modulation (PWM) for velocity and power factor control, as mentioned. The magnitude of the harmonic distortion depends mainly on the type of inverter or converter and its control because these use the IGBT thyristors (isolated gates bipolar transistors). The switching frequency in these inverters is limited to the range of 2 kHz to 3 kHz. The new turbines that now reach up to 5 MW of nominal power, the converters used are medium voltage, with a frequency of only 150 Hz to 250 Hz. As consequence, the frequency decrease being greater the distortion of the wave, or as it is the same, the emission of harmonic currents to the system is greater. These technologies cause harmonics (integer multiples of the fundamental frequency) and inter-harmonics (voltages or currents of frequencies that are not integer multiples of the system fundamental frequency which may appear as discrete frequencies or as a broadband spectrum) because they are loads that the dependence between the voltage and the current is not linear, therefore, it affects quality of the waveform, and can negatively affect other consumers connected to the electrical network.

Nowadays, a large variety of harmonic, inter-harmonic and subharmonic methods are employed to be synchronized with the fundamental component of the electrical network, thus avoiding the "leakage" effect with techniques based on the Discrete Fourier Transform (DFT), providing an optimum solution for the measurement of harmonics, inter-harmonics and sub-harmonics present in an electrical signal.

## **2. Wind Energy Conversion System – Squirrel cage induction machine**

Depending on the electric machine type being used as a generator, there are several configurations for the connection to the electrical network, these configurations have had an evolution over the years. Considering the different types of WECS configuration, the first one is based on a squirrel cage induction machine connected directly to the electrical network via a transformer as shown to **Figure 1**. The simplest configuration used in this type of wind turbine is the one that used soft-starter [1], [2] for the synchronization and connection to the network, being directly connected to it in a permanent operation. The squirrel cage induction machine is the cheapest machine, simple, robust and with less maintenance, which makes it very interesting for its application in wind generation. However, it has the disadvantage of the reactive power generation capacity, moreover, the

need to consume reactive power for its magnetization, in no-load and a full-load, which makes it necessary to use capacitor's bank

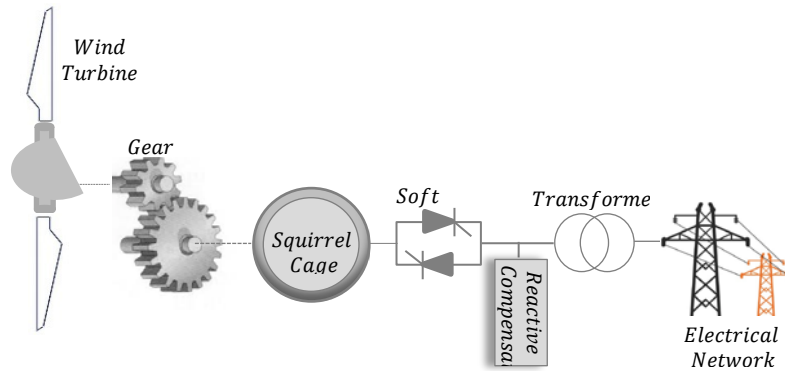


**Figure 1:** Asynchronous wind turbine connected to the electrical network

This configuration allows the power generation at constant frequency even when the velocity varies between 1 and 2% of the nominal velocity so this configuration is called “fixed-velocity” [3]. The machines with two windings are sometimes used, each with different number of pole pairs to work at two velocities. One of the windings with the lowest synchronization velocity is used for low power and the other with higher synchronization velocity for higher power [4]. Fixed-velocity wind turbines convert wind velocity fluctuations into mechanical fluctuations and these fluctuations in power regardless of the power control system used. In the case of weak networks, these fluctuations can cause voltage fluctuations at the connection point. For this reason, this configuration supposes a low insertion of the wind generation in electrical network, since it does not help to maintain the frequency stability in the network and leaves that work to the conventional synchronous generation.

### 2.1. Steady-state model of squirrel cage induction machine at fundamental frequency

The general configuration of induction machine in the stationary reference-frame is shown below which is obtained of a well-accepted model, with all the parameters referred to the stator, described by the circuit of **Figure 2** [5] which shows the model of a three-phase symmetrical induction machine [6]. Squirrel-cage induction machine is used in many industrial applications.

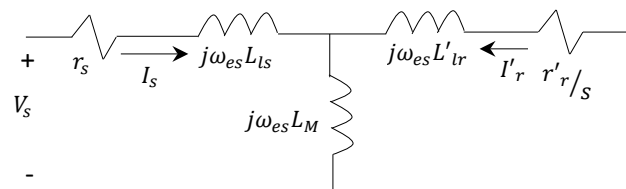


**Figure 2:** Steady-state equivalent circuit of the induction machine

The equation that describes the equivalent circuit is given by,

$$\begin{bmatrix} V_s \\ 0 \end{bmatrix} = \begin{bmatrix} r_s + j\omega_{es}(L_{ls} + L_M) & j\omega_{es}L_M \\ j\omega_{es}L_M & r'_r/s + j\omega_{es}(L'_{lr} + L_M) \end{bmatrix} \begin{bmatrix} I_s \\ I'_r \end{bmatrix} \quad (1)$$

Where  $V_s$  and  $V'_r$  are the stator and rotor phasor voltages,  $I_s$  and  $I'_r$  are the stator and rotor phasor currents, respectively, and  $L_M$  is the magnetizing inductance given by  $L_M = 3/2 L_{ms}$  and  $\omega_{es} = 2\pi f_{es}$  is the electric angular velocity and  $f_{es}$  is the frequency of the excitation source in the stator. The expression for the internal electromagnetic torque is,

$$T_e = \frac{V_s^2 (r'_r/s)}{(r_s + r'_r/s) + j\omega_{es}(L_{ls} + L_{lr})} \quad (2)$$

The electromagnetic torque and rotor velocity are related as follows

$$T_e = J \frac{2}{P} \frac{d\omega_{er}}{dt} + B_m \frac{2}{P} \omega_{er} + T_L \quad (3)$$

where  $J$  is the rotor inertia and of the connected load,  $\omega_{er}$  is the electric angular velocity,  $B_m$  is the damping coefficient associated with system load and the mechanical load. This parameter is typically small and often negligible, and  $T_L$  is the torque load. Additionally,  $s$  is the slip defined as

$$s = \frac{\omega_{es} - \omega_r}{\omega_{es}} \quad (4)$$

The slip of the induction machine is defined as the relative velocity between the magnetic field produced by the currents injected into the stator and the mechanical velocity of the rotor per unit of field velocity. In general, the field velocity is called the synchronous velocity of the machine and the slip indicates how close the machine is to this velocity. **Figure 3** shows the relationship between the rotor velocity and the induced torque generates by the machine.

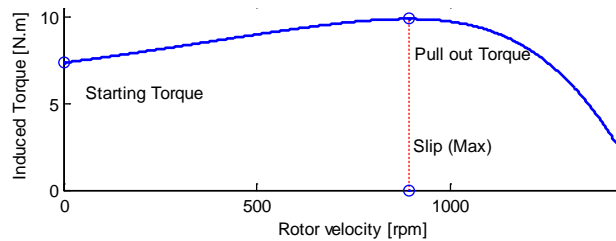


**Figure 3:** Maximum slip in relation to rotor velocity and induced torque.

The slip values describe the operation of the induction machine as follows: the slip is positive if  $\omega_{es} > \omega_r$  which means that the machine is operating as a motor, the slip is negative if  $\omega_{es} < \omega_r$  when the machine is operating as a generator, the slip is 1 if  $\omega_r = 0$  when the machine has the rotor blocked and works as a transformer, and finally the slip is zero if  $\omega_{es} = \omega_r$  when the machine is rotating but the torque is zero (unloaded).

If it is a squirrel cage, then the rotor is short-circuited, at that moment a current is induced in the rotor with an angular velocity  $\omega_{er} = \omega_{es} - \omega_r$  or an electric frequency of  $f_{er} = \omega_{er}/2\pi$ . This frequency can be expressed as a function of the slip and the stator frequency:

$$f_{er} = sf_{es} \tag{4}$$

However, if the rotor is fed with a source of frequency  $f_{er}$  it will induce a current in the stator of frequency,

$$f_{es} = f_{er}/s \tag{5}$$

The phasors current are obtained solving (1), i.e.,  $I_s = |I_s|\angle\varphi_s$  and  $I'_r = |I'_r|\angle\varphi_r$ . Their representations in the time domain in their respective windings are,

$$i_s = |I_s| \cos(\omega_{es}t + \varphi_s) \tag{6}$$

$$i_r = |I'_r| \cos(s\omega_{es}t + \varphi'_r - \theta_{ef})$$

where  $\theta_{ef}$  is the phase angle between the rotor and stator in steady-state. The relation between the angular velocity and the angular displacement is the angle obtained from  $\theta_r = \int_0^t \omega_r(\xi)d\xi + \theta_r(0)$  where  $\xi$  is a dummy variable of integration. In addition, in steady-state results in  $\theta_r = \omega_r t + \theta_{ef}$  and then:

$$\theta_{ef} = \theta_r - \omega_r t \tag{7}$$

If the analysis is developed seen from rotor, then the machine inductances are in function of rotor velocity, which describe the machine behavior to be varying in time. For this is necessary a change of variables to the desired reference-frame to avoid the complexity of the differential equations. The general transformation refers the machine variables to a reference-frame, which rotates at any arbitrary angular velocity. Assuming that the machine operates under balanced conditions, the stator and rotor quantities are zero knowing that for steady-state conditions the variables  $d$  and  $q$  are sinusoidal in all reference-frames except the rotating synchronous reference frame where they are constant. The general configuration of induction machine seen from rotor in the stationary reference-frame is shown in **Figure 4** with all the parameters referred to the rotor, which shows the model of a three-phase symmetrical induction machine.

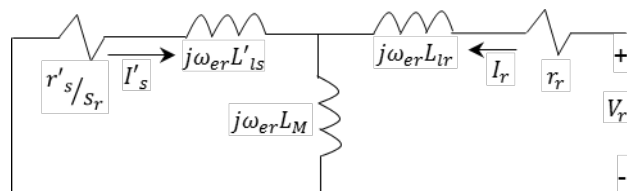


**Figure 4:** Steady-state equivalent circuit induction machine seen from rotor

The equation that describes the system is given by (as seen from the rotor)

$$\begin{bmatrix} 0 \\ V_r \end{bmatrix} = \begin{bmatrix} r'_s/s_r + j\omega_{er}(L'_{ls} + L_M) & j\omega_{er}L_M \\ j\omega_{er}L_M & r_r + j\omega_{er}(L_{lr} + L_M) \end{bmatrix} \begin{bmatrix} I'_s \\ I_r \end{bmatrix} \quad (8)$$

Since the rotor is moving, the slip seen from the rotor is given by:

$$s_r = \frac{\omega_{er} + \omega_r}{\omega_{er}} \quad (9)$$

Now, the phasors current are obtained of (8), i.e.,  $I_r = |I_r|\angle\varphi_r$  and  $I'_s = |I'_s|\angle\varphi_s$ . Their representations in the time domain, in their respective windings, are

$$i_r = |I_r| \cos(\omega_{er}t + \varphi_r) \quad (10)$$

$$i_s = |I'_s| \cos(s_r\omega_{er}t + \varphi'_s + \theta_{ef})$$

**2.2. Steady-state model of squirrel cage induction machine at harmonics frequency**

When the induction machine is fed by non-sinusoidal voltages and currents, the magnetic field in the air-gap and the rotor currents contain components at harmonic frequencies. This harmonics can be positive, negative and zero sequence. The positive sequence harmonics (1, 4, 7, 10, 13, etc.) produce magnetic fields and currents that rotate in the same direction as the fundamental frequency. For the current system (consisting of the fundamental and 5<sup>th</sup> harmonic components where the 5<sup>th</sup> harmonic system rotates in counterclockwise direction) the fifth time harmonic has the angular velocity  $d\theta_5/dt = -5\omega_f$ . Phasor representation for forward rotating fundamental and forward rotating 5<sup>th</sup> harmonic current system is given in **Figure 5**.

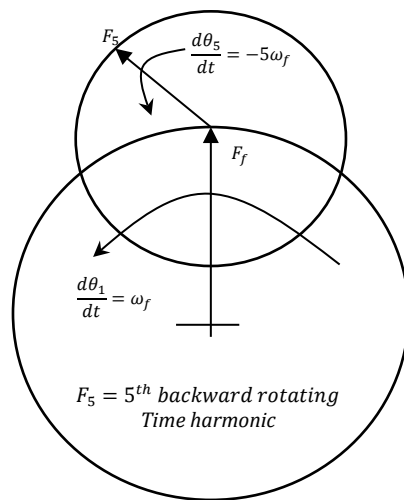


**Figure 5:** Forward (+) rotating fundamental mmf of an induction machine superposed with forward (+) rotating 5<sup>th</sup> time harmonic rotating in the same direction.

The negative sequence harmonics (2, 5, 8, 11, 14, etc.) develop magnetic fields and currents that rotate in the opposite direction of the fundamental. Zero sequence harmonics (3, 9, 15, 21, etc.) do not develop a useful torque, but cause additional losses in the induction machine. Only wye-connections with insulated neutral and delta are used to connect the stator winding. From this, it follows that in these induction machines with zero sequence there are no homopolar currents in the stator winding. Similar analysis can be performed to determine the rotating directions of each individual time harmonic and to define the positive-, negative-, and zero sequence harmonic orders, as listed in Table 1.

**Table 1:** Positive, negative and zero sequence time harmonics

<b>Time-harmonic sequence</b>	<b>+</b>	<b>-</b>	<b>0</b>
Time-harmonic order	1	2	3
	4	5	6
	7	8	9
	10	11	12
	13	14	15
	⋮	⋮	⋮

Considering that the machine is fed from the stator with a harmonic voltage source while the rotor is short-circuited. This machine has a well-adopted steady-state model [7], with all parameters referred to the stator, described by the circuit of **Figure 6**.

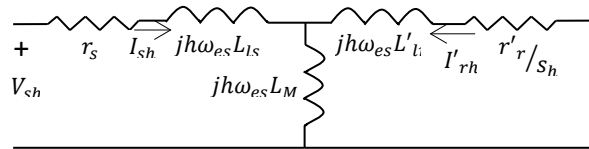


**Figure 6:** Steady-state harmonic equivalent circuit of the induction machine

The equation that then represents the circuit is:

$$\begin{bmatrix} V_{sh} \\ 0 \end{bmatrix} = \begin{bmatrix} r_s + jh\omega_{es}(L_{ls} + L_M) & jh\omega_{es}L_M \\ jh\omega_{es}L_M & r'_r/s_h + jh\omega_{es}(L'_{lr} + L_M) \end{bmatrix} \begin{bmatrix} I_{sh} \\ I'_{rh} \end{bmatrix} \tag{11}$$

The equation that determinates the slip of the induction machine at harmonic frequency is,

$$s_h = \frac{\pm h\omega_{es} - \omega_r}{\pm h\omega_{es}} \tag{12}$$

The sign ( $\pm$ ) is used for positive or negative sequence, respectively. In this case the harmonics with positive sequence behavior are  $h = 3k + 1$  and negative  $h = 3k - 1$  for  $k = 1,2,3, \dots$  where the most common harmonics are the 5,7,11,13,15,17,... known as the characteristic harmonics. The harmonic phasors current are obtained of (11), i.e.  $I_{sh} = |I_{sh}| \angle \varphi_{sh}$  and  $I'_{rh} = |I'_{rh}| \angle \varphi'_{rh}$ . Their representations in the time domain, in their respective windings are,

$$i_{sh} = |I_{sh}| \cos(h\omega_{es}t + \varphi_{sh}) \tag{13}$$

$$i_{rh} = |I'_{rh}| \cos(s_h h\omega_{es}t + \varphi'_{rh} \mp \theta_{ef})$$

The mathematical analysis developed is implemented in an algorithm in MATLAB/Simulink. To validate the proposed model for harmonic analysis, in steady state, of the squirrel cage induction machine, it is necessary to compare it with the induction machine model in dynamic-state. This same analysis and modeling are developed in the MATLAB/Simulink computer platform. It is necessary to mention that both results are compared once the model in dynamic-state reaches its stable value. Considering that, the induction machine is fed from the stator with a sinusoidal voltage source  $V_s$  and the rotor is short-circuited, then the phasor currents in the stator and rotor winding are obtained. The synchronous velocity of the machine and the electromagnetic torque are also determined. The characteristics of the machine are 50 HP/37.3 kW, 4-pole, at 60 Hz and 46.8 A, at a nominal velocity of 1705 rpm.

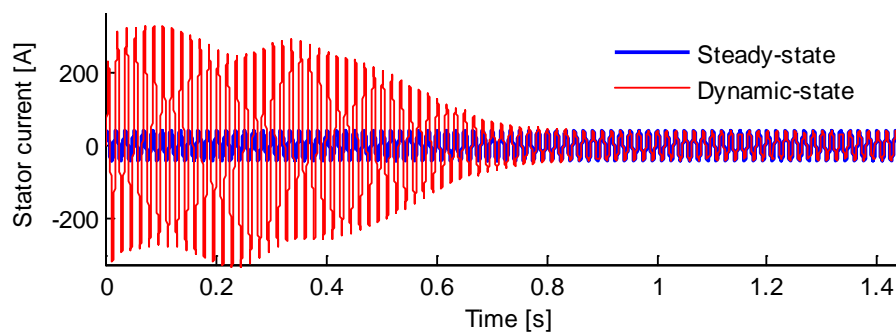


**Figure 7:** Stator current

The parameters of the induction machine are shown in Table 2. The voltage at which the machine is fed is 120 V at 60 Hz. The stator and rotor currents modeled in both states are shown in **Figure 7** and **10**, respectively. In this case, a mechanical torque of 198 N × m is considered.

**Table 2:** Induction machine parameters

Parameters	50 HP/37.3 kW
Number of poles	4
Inertia	1.662 kg·m <sup>2</sup> .
Nominal line current	46.8 Amps
Nominal line-to-line voltage	460 V <sub>rms</sub>
Nominal torque	198 N.m
Nominal frequency	60 Hz
Stator resistance, $r_s$	0.087Ω
Stator inductance, $L_{ls}$	8 H
Rotor resistance, $r_r$	0.034 Ω
Rotor inductance, $L_{lr}$	8 H
Magnetizing inductance, $L_{mr} = L_{ms}$	155 H
Rotor speed	1705 rpm

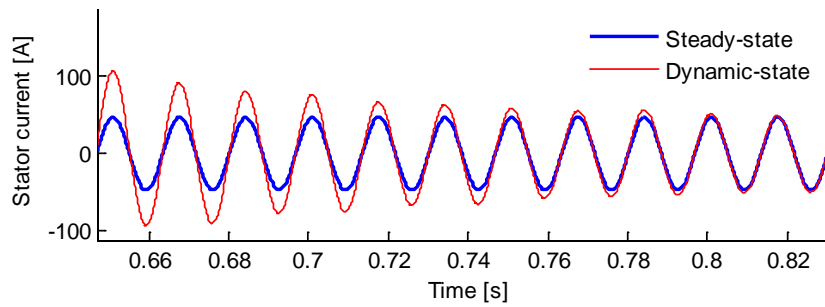


**Figure 8:** Zoom of the Figure 11

**Figure 8** shows the stator current, in dynamic-state, reaching the stable moment (red line) and comparing with the stator current modelled in steady-state (blue line). In 0.8 seconds, both waveforms of the stator current are compared in magnitude and phase angle and it is observed that they behave in the same way by validating the proposed model in steady-state of the induction machine. The system frequency is 60 Hz, which are observed in **Figure 9**.

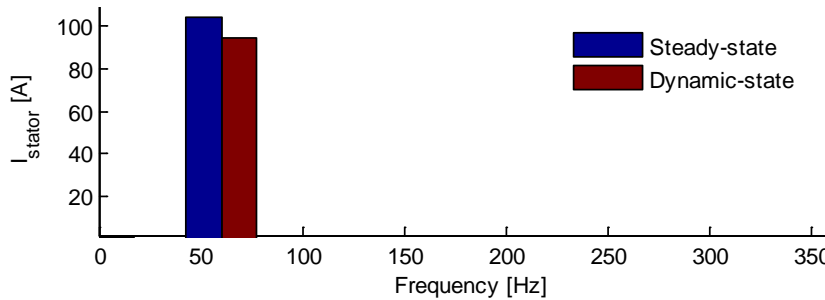


**Figure 9:** Stator frequencies

In this figure the frequency of the induction machine, in the dynamic-state (red bar), and steady-state (blue bar) is observed where the similarity in the magnitude of the frequency in both states are analyzed. Additionally, for this study case, the values of the simulation are: slip,  $s = 0.0464$  and the stator power is,  $P_s = 3,780 W$ . This same procedure is performed for the rotor winding where in **Figure 10** the rotor current of phase A is shown in dynamic-state, this being compared to the rotor current in steady-state. Both behaviors coincide with magnitude and phase when the current in dynamic-state reaches its stable value. The **Figure 11** shows the system frequency in the rotor.

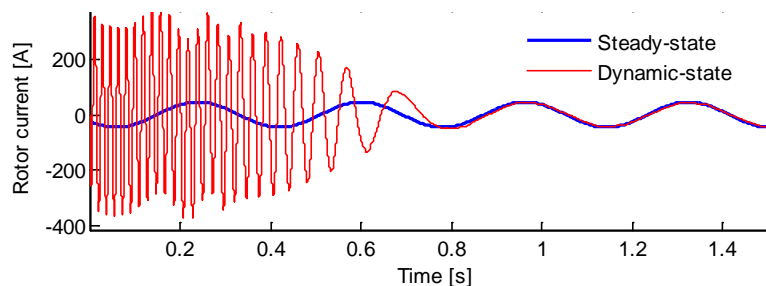


**Figure 10:** Rotor current

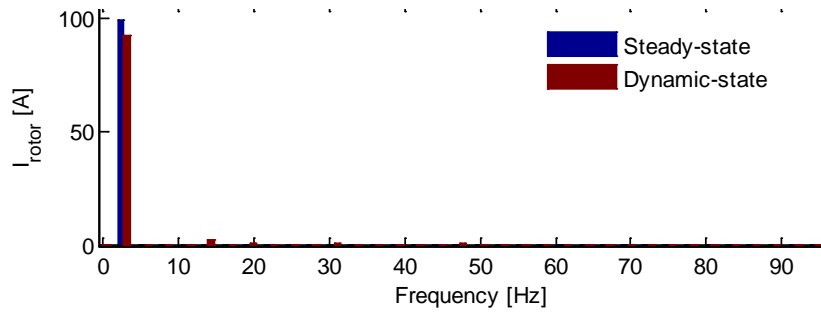


**Figure 11:** Rotor frequencies

The electromagnetic torque and the velocity of the induction machine are shown in **Figure 12** and **Figure 13**, respectively and it is observed that the torque that develops in the machine tends to zero in a very habitual behavior when the machine is only fed by the stator. It is also observed that the machine quickly reaches its rated velocity (0.7 sec) because it is operating under normal operating conditions.

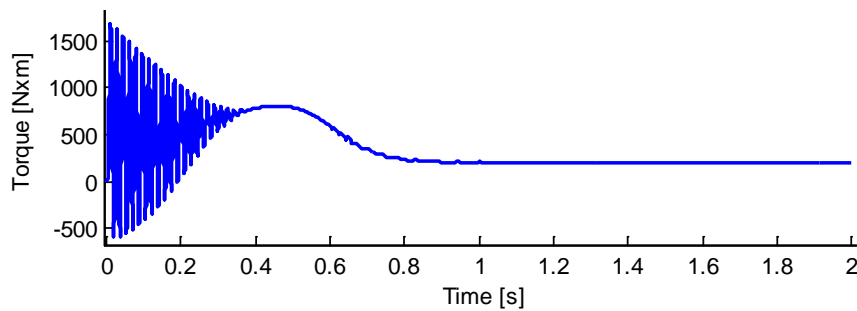


**Figure 12:** Torque of the induction machine

With the increase in the use of non-linear loads (from power electronics), problems have started to occur, due to the generation of harmonic currents and voltages in the electrical power system. These include: overheating of cables, transformers and induction machines, excessive currents in the neutral, phenomena of resonance between circuit elements, etc. Increasing harmonic voltage distortion can cause malfunctioning of many equipment (especially the less robust ones) that have been designed to operate under normal conditions.

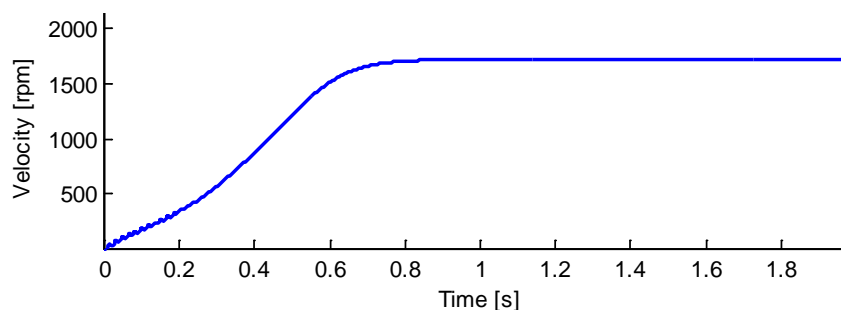


**Figure 13:** Velocity of the induction machine

In power systems, induction machines are a very representative component of the load and are widely used in

industrial and commercial installations. Induction machines are sensitive to harmonics and are subjected to all kinds of variations of the power source, which affects their characteristics of operation. If it is considered that, the induction machine is fed from the stator with a harmonic voltage source  $V_{sh}$  with frequency  $f_{sh}$  being the rotor short-circuited. The voltage source is 460 V at 60 Hz in the stator, which includes the third, fifth, and seventh harmonics. The magnitudes and angles of the components of the harmonic voltage are shown in Table 3.

**Table 3:** Harmonic components of the stator voltage

	Fundamental	Third	Fifth	Seventh
<b>Magnitude</b>	460	153.3	92	65.714
<b>Angle</b>	30°	113°	42.85°	137.15°

The three-phase harmonic voltage with which it is excited to the stator winding of the induction machine is shown in **Figure 14**. This voltage waveform is obtained of (11) and the harmonic equivalent circuit of the induction machine shown in Figure 6.

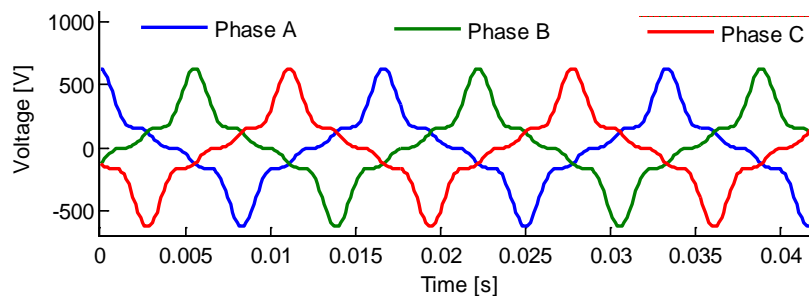


**Figure 14:** Stator voltage

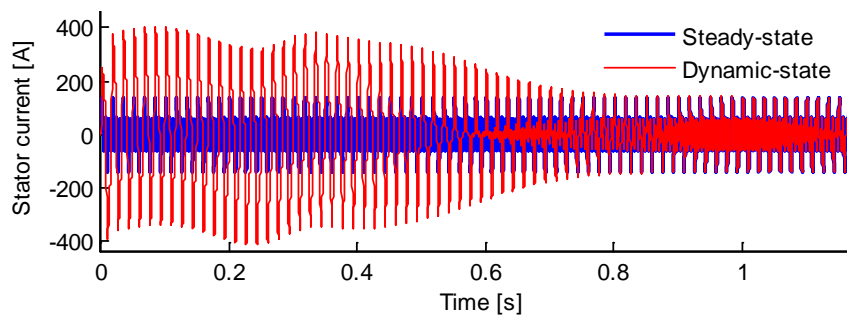


**Figure 15:** Stator current

The stator and rotor currents modeled in both states are shown in **Figure 15** and **Figure 17**, respectively. In this case, a mechanical torque of  $198 \text{ N} \times \text{m}$  is considered. **Figure 16** shows an enlargement of Figure 15 in which the moment is observed where both modeling of the machine coincide in magnitude and angle verifying the

efficiency of the proposed model, in steady-state, for studies of propagation of harmonics.

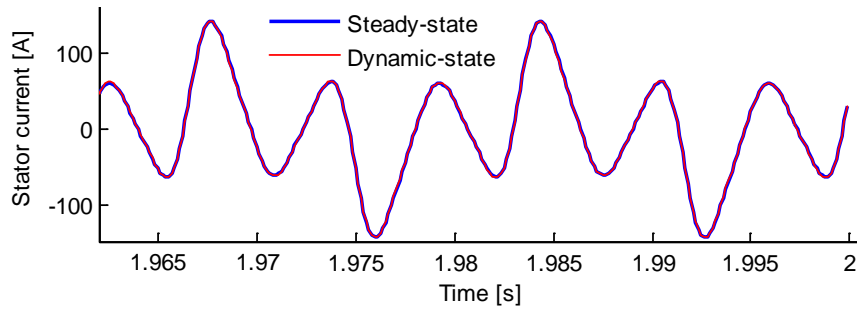


Figure 16: Zoom of the Figure 15

Figure 17 shows the rotor current in dynamic-state. Once this reaches its stable value is compared to the rotor current of the proposed model in steady-state observing that after 1 second both models can be compared in magnitude and phase angle observing the same waveform. Figure 18 shows an enlargement of the Figure 17.

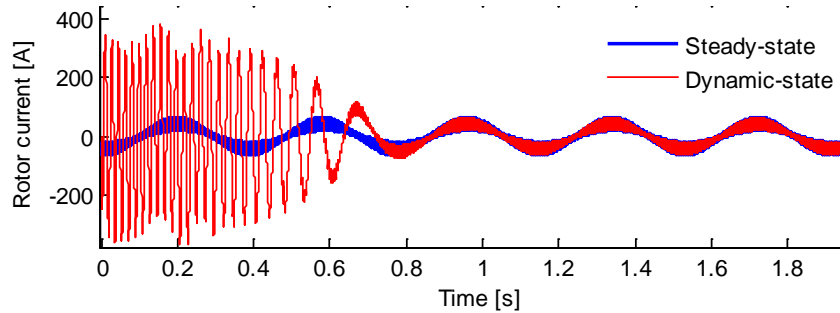


Figure 17: Stator current

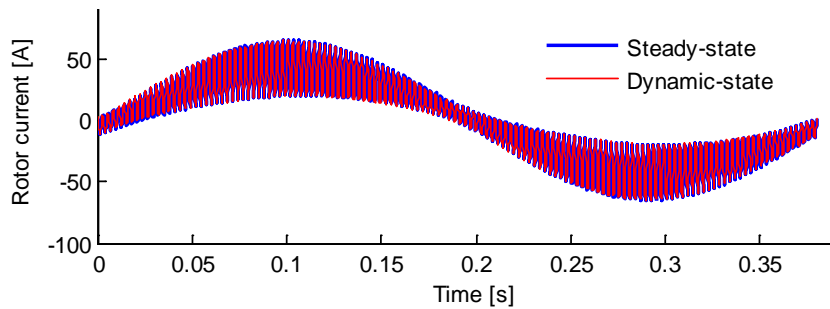


Figure 18: Zoom of the Figure 17

For this study case, the harmonic slip for the positive, negative and zero sequences components, will be equal to:

Positive sequence:

$$s_{h(+)} = \frac{h\omega_{es} - \omega_r}{h\omega_{es}} \quad (14)$$

Negative sequence:

$$s_{h(-)} = \frac{h\omega_{es} + \omega_r}{h\omega_{es}} \tag{15}$$

In according to eqs (14) and (15), the harmonic slip, in positive and negative sequence, will be:

$$s_{h(-)} = \frac{h\omega_{es} + \omega_r}{h\omega_{es}} = \frac{5 \times 1800 + 1200}{5 \times 1800} = \mathbf{1.1333}$$

$$s_{h(+)} = \frac{h\omega_{es} - \omega_r}{h\omega_{es}} = \frac{7 \times 1800 - 1200}{7 \times 1800} = \mathbf{0.9047}$$

The frequencies induced in the winding of the rotor are obtained with:

$$f_r = \frac{s_h \times h \times \omega_{es}}{2\pi} \tag{16}$$

Then, the fundamental frequency that the stator winding induces the rotor winding, according to (16),

$$\frac{s_h \times h \times \omega_{es}}{2\pi} = \frac{0.332 \times 1 \times 377}{2\pi} = \mathbf{20 \text{ Hz}}$$

The fifth harmonic inducing the stator winding to the rotor winding will be

$$\frac{s_5 \times h \times \omega_{es}}{2\pi} = \frac{1.333 \times 5 \times 377}{2\pi} = \mathbf{360 \text{ Hz}}$$

Finally, the seventh harmonic, inducing the stator winding to the rotor winding, will be

$$\frac{s_7 \times h \times \omega_{es}}{2\pi} = \frac{0.9047 \times 7 \times 377}{2\pi} = \mathbf{380 \text{ Hz}}$$

These frequencies can be observed in **Figure 19** and **Figure 20** in which are shown the induced frequencies of the stator to the rotor, respectively, in according with the previous analysis.

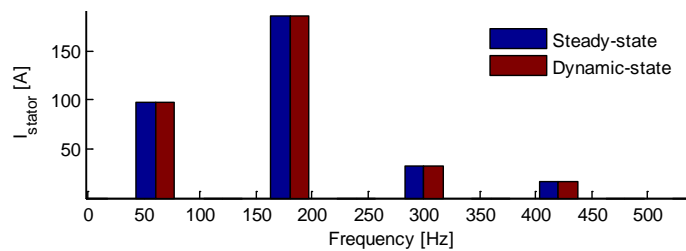


**Figure 19:** Stator frequencies

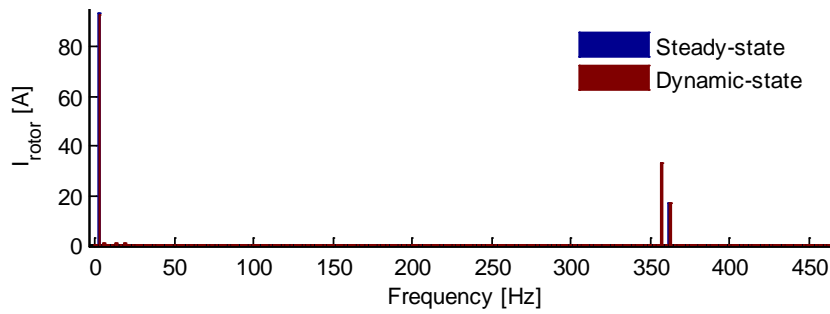


**Figure 20:** Rotor frequencies

These frequencies induced in the rotor cannot be called harmonic frequencies since they are not integral multiples of the fundamental frequency but it should be noted that they are the 17th and 19th harmonic of the fundamental frequency of the rotor. The electromagnetic torque and the velocity of the induction machine under harmonics operating conditions are shown in **Figure 21** and **Figure 22**, respectively and it is observed that the torque that develops in the machine present harmonic content when the machine is fed by the harmonic voltage. It is also observed that the machine it takes time to reach its rated velocity in this conditions operating.

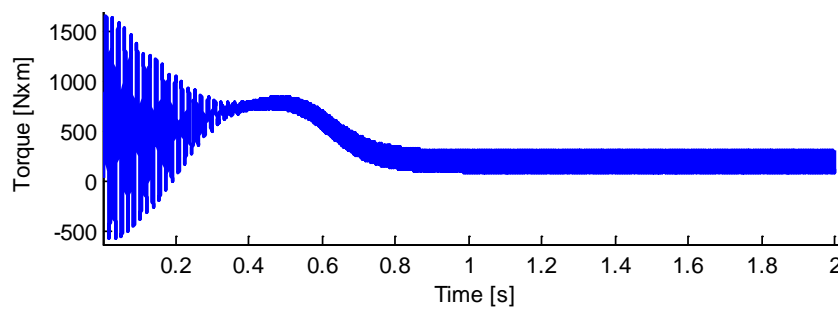


**Figure 21:** Electromagnetic torque of the induction machine in harmonic conditions of operation.

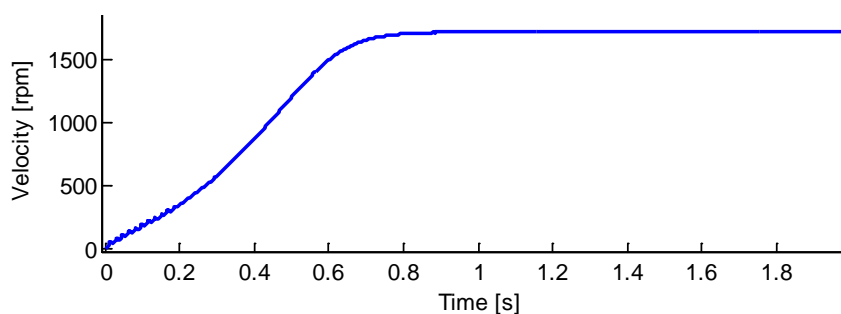


**Figure 22:** Velocity of the induction machine

### 3. Wind Energy Conversion System – Doubly-fed induction machine

In this configuration, known as a double-fed wind turbine, the rotor is connected to the electrical network via a

frequency converter while the stator is connected directly to the electrical network via a transformer as shown in **Figure 23**. With this configuration, it is possible to control the active and reactive power [8], with low levels of harmonics both on the generator and on the electrical network side. The performance is limited by the size of the equipment. For a power equipment of 25% of the rated power of the machine, the speed variation is around  $\pm 33\%$  [9]. In addition, it has the advantage of delivering over-rated power to the electrical network at super-synchronous operating velocities [8]. The size required for the converter in this configuration makes it very economically attractive. Its main disadvantage is the use of brushes and the need for additional protection in case of faults in the electrical network. A dip of voltage in the network causes an increase in stator current, and due to the magnetic coupling between stator and rotor windings, this current will also flow through the rotor and the power equipment can destroy it [10]. This requires additional equipment such as the so-called "active crowbar". In the technology, a double-fed induction generator with wound rotor (DFIG) is used. Although its axis rotates at variable velocity, the DFIG can generate a constant frequency voltage when the rotor windings are fed with a frequency converter. This converter consists of two reversible AC/DC electronic converters connected to each other via a DC bus.

The converter connected to the rotor regulates the amplitude, frequency and phase sequence of the voltage applied to the rotor, allowing a vector control of the machine to regulate the electromagnetic torque and the power factor of the generator over a wide velocity range of rotation [11], [12].

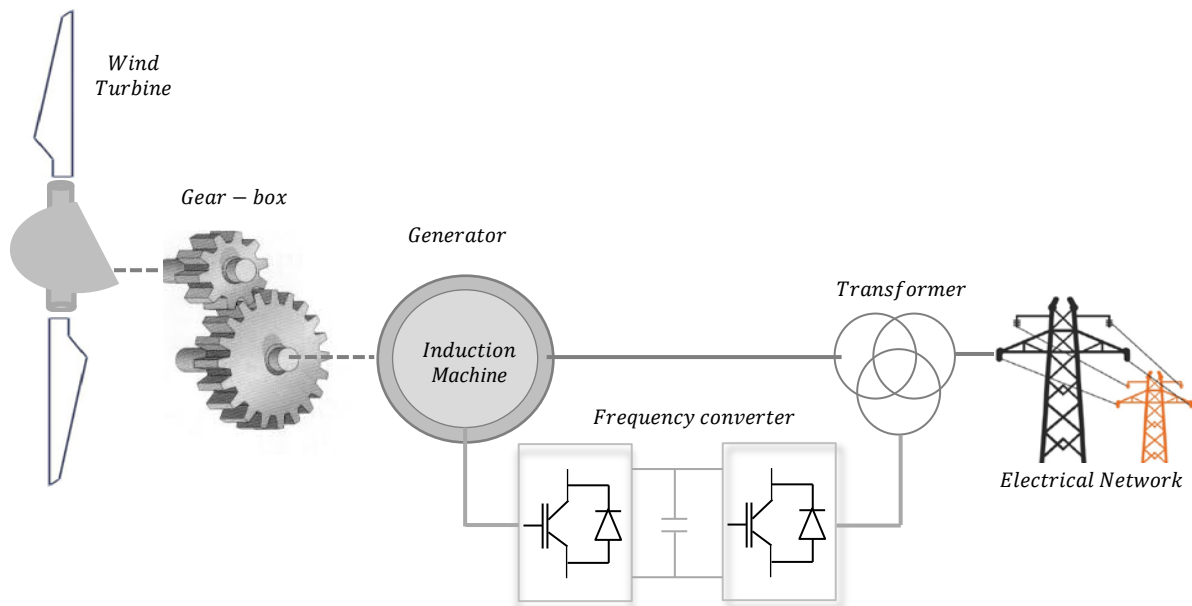


**Figure 23:** Asynchronous wind turbine connected to the electrical network

### 3.1. Steady-state model of doubly-fed induction machine at fundamental frequency

In DFIG, the rotor is connected to the electrical network via a frequency converter and the stator is connected directly to the network. This topology can generate a stator voltage  $V_s$  of angular frequency  $\omega_{e_s}$  is constant, whereas by the rotor the voltage  $V_r$  of angular frequency  $\omega_r$  variable. At velocity  $\omega_r$  is known as relative

velocity or slip. According to the fundamental principle of rotating electric machines with respect to the angular frequencies of magnetic fields between stator and rotor windings, to develop a pair with a value other than zero [13], and considering that the number of pole pairs  $P$  is same in both windings, it is,

$$\omega = \omega_{es} \pm \omega_r \tag{17}$$

Since  $\omega$  is the electric angular velocity of the rotor, which is defined as,

$$\omega = P \pm \omega_m \tag{18}$$

where  $\omega_m$  is the mechanical angular velocity or rotation of the rotor. The velocity  $\omega$  may be greater or less than  $\omega_{es}$ . In the case where  $\omega < \omega_{es}$ , the velocity  $\omega_r$  is positive in (17), and the DFIG is capable to operate at sub-synchronous velocity. On the other hand, if in  $\omega > \omega_r$  the velocity  $\omega_r$  is negative then the DFIG will operate at super-synchronous velocity. A general configuration of a DFIG uses a wound rotor with slip rings to transmit current between the stator and rotor voltage sources. This machine has a well-adopted steady-state model, with all the parameters referred to the stator described by **Figure 24**. The voltage equation that describes the equivalent circuit is given by:

$$\begin{bmatrix} V_s \\ \frac{1}{s}V'_r \end{bmatrix} = \begin{bmatrix} r_s + j\omega_{es}(L_{ls} + L_M) & j\omega_{es}L_M \\ j\omega_{es}L_M & r'_r/s + j\omega_{es}(L'_{lr} + L_M) \end{bmatrix} \begin{bmatrix} I_s \\ I'_r \end{bmatrix} \tag{19}$$

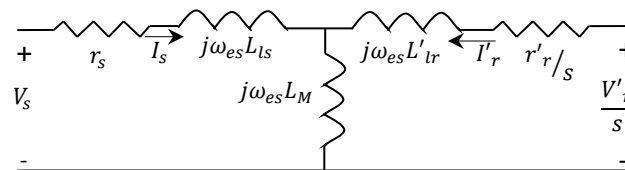


**Figure 24:** Equivalent circuit in steady-state of the induction machine

The parameters and variables of this equivalent circuit were described in the previous section. Now, if the rotor is short-circuited, a current is induced in the rotor at an angular frequency  $\omega_{er} = \omega_{es} - \omega_r$  or at an electric frequency of  $f_{er} = \omega_{er}/2\pi$ . This is important when the induction machine is double fed, for example if a machine has a slip of 0.2 and is fed from the stator at a frequency of 60 Hz, it induces a frequency of 12 Hz in the rotor and if the rotor is also fed with a frequency of 7 Hz, it will also induce a frequency of 35 Hz in the stator. Therefore, the stator will have a current with two components, one at 60 Hz and other at 35 Hz and the rotor will have one of 6 Hz and other of 12 Hz. It is common for a doubly fed induction machine with a constant frequency in the rotor, which will induce different frequencies in the stator depending on the slip values. These frequencies are called inter-harmonic, since they are not integer multiples of the fundamental frequency  $f_{es}$ .

Considering that, the doubly fed induction machine is fed from the stator with a voltage source  $V_s$  of frequency  $f_{es}$  with the short-circuited rotor. The phasors current, in their representations in the time domain, for their respective windings are [14],

$$i_s = |I_s| \cos(\omega_{es}t + \varphi_s) \tag{20}$$

$$i_r = |I'_r| \cos(s\omega_{es}t + \varphi'_r - \theta_{ef})$$

Considering the opposite case, the DFIG is fed from the rotor with a voltage source  $V_r$  of frequency  $f_{er}$  and stator in short-circuit. If the rotor is in motion, the slip seen from the rotor is given by,

$$s_{rh} = \frac{\pm h\omega_{er} + \omega_r}{\pm h\omega_{er}} \tag{21}$$

The sign (+) is used for positive and (-) for negative sequence, respectively. A simple analysis to verify this, for example, if the rotor is fed with a frequency  $\omega_{er} = s\omega_{es}$  from where  $\omega_r = \omega_{es}(1 - s)$ , then from this results in  $s_r = 1/s$ , that is, the induced frequency in the stator is  $f_{es} = s_r f_{er} = f_{er}/s$  which is in agreement with (5). The phasors current in their representations in the time domain, in their respective windings, are

$$i_r = |I_r| \cos(\omega_{er}t + \varphi_r) \tag{22}$$

$$i_s = |I'_s| \cos(s_r\omega_{er}t + \varphi'_s + \theta_{ef})$$

The complete solution for the DFIG is given by the sum of the two effects, i.e.,

$$i_s = |I_s| \cos(\omega_{es}t + \varphi_s) + |I'_s| \cos(s_r\omega_{er}t + \varphi'_s + \theta_{ef}) \tag{23}$$

$$i_r = |I_r| \cos(\omega_{er}t + \varphi_r) + |I'_r| \cos(s\omega_{es}t + \varphi'_r - \theta_{ef})$$

It should be noted that both currents are sinusoidal only if the voltage source in the rotor has a frequency  $f_{er} = sf_{es}$ .

### 3.2. Steady-state model of doubly-fed induction machine at harmonic frequency

In an doubly-fed induction machine, the harmonics are generated on both windings: harmonics in the stator voltage source with frequencies  $f_{sh} = hf_{es}$  and harmonics in the rotor voltage source with frequencies  $f_{rh} = hf_{er}$ , where  $h$  is an integer. The induced frequencies in the rotor, however, due to harmonics in the stator, are inter-harmonics of the rotor fundamental frequency and vice versa.

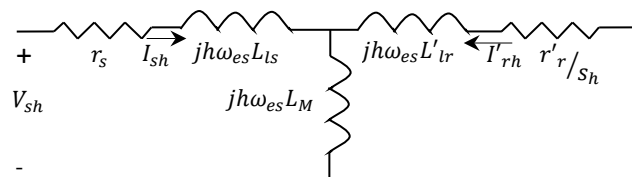


**Figure 25:** Harmonic equivalent circuit in steady-state of DFIG seen from the rotor

Considering that the machine is fed from the stator with a source of harmonic voltage of frequency  $hf_{es}$ , being the rotor in short-circuit. This machine has a well-adopted steady-state model, with all parameters referred to the stator, described by the circuit of **Figure 25**. The equation that represents the circuit is,

$$\begin{bmatrix} 0 \\ V_{rh} \end{bmatrix} = \begin{bmatrix} \frac{r'_s}{s_{rh}} + jh\omega_{er}(L'_{ls} + L_M) & jh\omega_{er}L_M \\ jh\omega_{er}L_M & r_r + jh\omega_{er}(L_{lr} + L_M) \end{bmatrix} \begin{bmatrix} I'_{sh} \\ I_{rh} \end{bmatrix} \quad (24)$$

The phasors current in their representations in the time domain, in their respective windings, are

$$i_{rh} = |I_{rh}| \cos(h\omega_{er}t + \varphi_{rh}) \quad (25)$$

$$i_{sh} = |I'_{sh}| \cos(s_{rh}h\omega_{er}t + \varphi'_{sh} \pm \theta_{ef})$$

The complete solution for the DFIG is given by the sum of the two effects, i.e.,

$$i_{sh} = |I_{sh}| \cos(h\omega_{es}t + \varphi_{sh}) + |I'_{sh}| \cos(s_{rh}h\omega_{er}t + \varphi'_{sh} \pm \theta_{ef}) \quad (26)$$

$$i_{rh} = |I_{rh}| \cos(h\omega_{er}t + \varphi_{rh}) + |I'_{rh}| \cos(s_h h\omega_{es}t + \varphi'_{rh} \mp \theta_{ef})$$

The slip's equation, (12) and (21), are used are only valid under balanced conditions, for positive and negative sequences. To an analysis of zero sequence, the induction machine works as two-decoupled windings, resulting in the circuit of **Figure 26**,

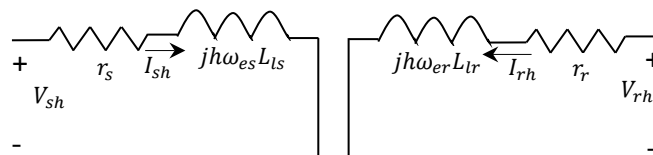


**Figure 26:** Induction machine triplex harmonic model seen from stator and rotor

The equation that represents the circuit is

$$V_{sh} = (r_s + jh\omega_{es}L_{ls})I_{sh} \quad (27)$$

$$V_{rh} = (r_r + jh\omega_{er}L_{lr})I_{rh}$$

The phasors current are obtained of (27) in their representations in the time domain, in their respective windings, are

$$i_{sh} = |I_{sh}| \cos(h\omega_{es}t + \varphi_{sh}) \quad (28)$$

$$i_{rh} = |I_{rh}| \cos(h\omega_{er}t + \varphi_{rh})$$

Now the general solution for balanced conditions including voltage sources at fundamental and harmonic frequencies in the stator and rotor is given by

$$i_s = \sum_{h=1}^H |I_{sh}| \cos(h\omega_{es}t + \varphi_{sh}) + \sum_{h=1,3k+1}^H |I'_{sh}| \cos(s_{rh}h\omega_{er}t + \varphi'_{sh} + \theta_{ef}) + \sum_{h=3k-1}^H |I'_{sh}| \cos(s_{rh}h\omega_{er}t + \varphi'_{sh} - \theta_{ef}) \tag{29}$$

$$i_r = \sum_{h=1}^H |I_{rh}| \cos(h\omega_{er}t + \varphi_{rh}) + \sum_{h=1,3k+1}^H |I'_{rh}| \cos(s_h h\omega_{es}t + \varphi'_{rh} - \theta_{ef}) + \sum_{h=3k-1}^H |I'_{rh}| \cos(s_h h\omega_{es}t + \varphi'_{rh} + \theta_{ef}) \tag{30}$$

These equations are given for the proposed doubly-fed induction machine model. Below is a brief explanation: all the current harmonics included positive-, negative-, and zero-sequence harmonics (first summation of 29). All the current harmonics because of the induction effect of the positive-sequence voltage source harmonics in the rotor (second summation of 29) and all the current harmonics because of induction effect of the negative-sequence voltage source harmonics in the rotor (third summation of 29). The same interpretation is for (30).

Considering that, the induction machine is fed from the stator with a sinusoidal voltage source  $V_s$  and the rotor is fed from the rotor with a sinusoidal voltage source  $V_r$  too. The characteristics of the machine are: 50 HP/37.3 kW, 4-pole, at 60 Hz and 46.8 A, at a nominal velocity of 1705 rpm. The parameters of the induction machine are shown in Table 2. The voltage at which the machine is fed is 460 V at 60 Hz and the rotor voltage is 50 V. The stator and rotor currents modeled in both states are shown in **Figure 27** and **Figure 29**, respectively, where they show the behavior of the stator current, in dynamic-state and steady-state. At the end, both waveforms of the stator current are compared in magnitude and phase angle and it is observed that they behave in the same way by validating the proposed model in steady-state of the induction machine. A mechanical torque of  $198 \text{ N} \times \text{m}$  is also used for this case study.

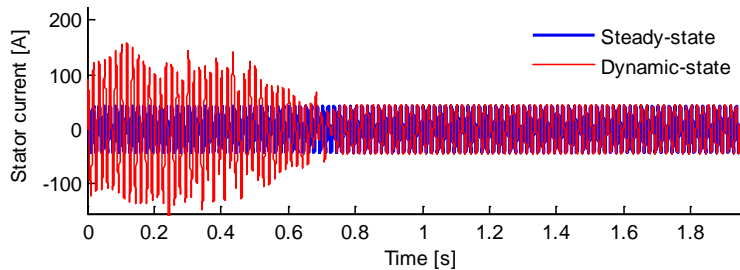


**Figure 27:** Stator current

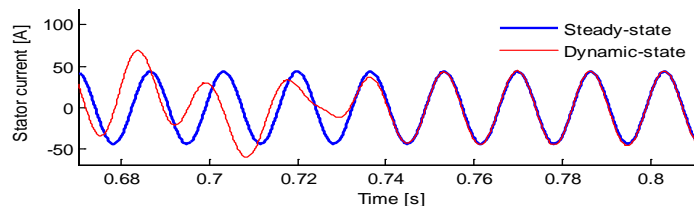


**Figure 28:** Zoom of the Figure 27

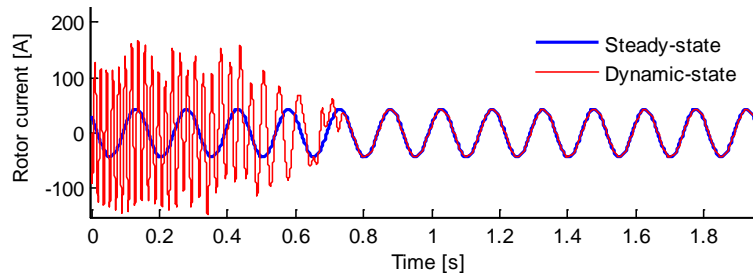


Figure 29: Rotor current

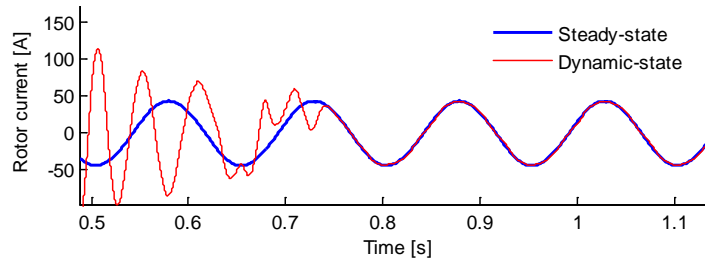


Figure 30: Zoom of the Figure 33

Figure 31 and Figure 32 show the induced frequencies of the stator to the rotor and vice versa. According to the analysis previously demonstrated, the machine is excited, on the stator side, to a voltage  $V_s$  at 60 Hz.

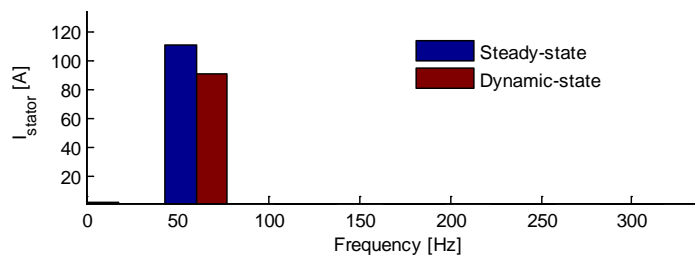


Figure 31: Stator frequency

Considering that the machine has a slip,  $s = 0.1$ , then a current component is generated at 6 Hz, as  $f_r = sf_{es} = 0.1 \times 60 = 6 \text{ Hz}$  verifying that both, stator and rotor, generate current with two components each: the own frequency and the induced frequency of the other winding. The electromagnetic torque and the velocity of the induction machine under normal operating conditions are shown in Figure 33 and Figure 34, respectively.

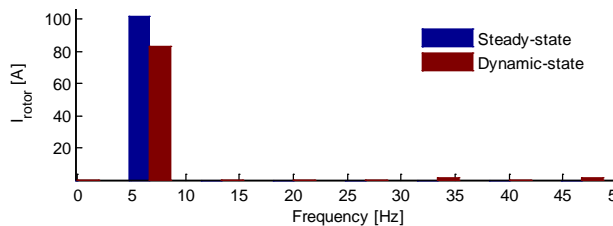
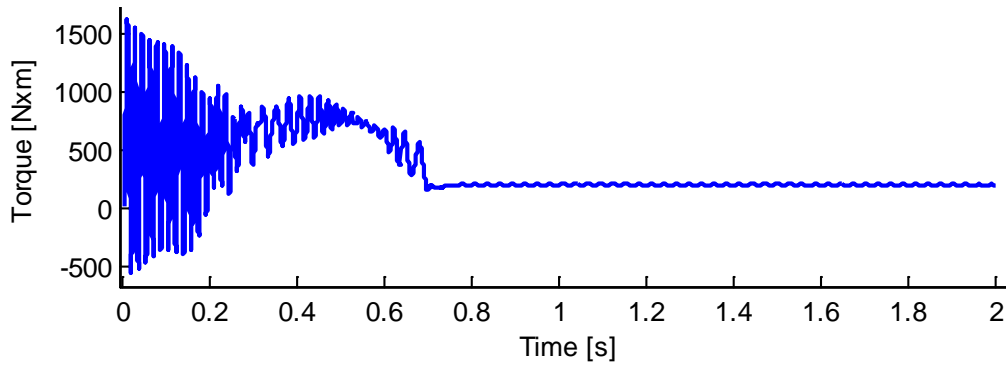
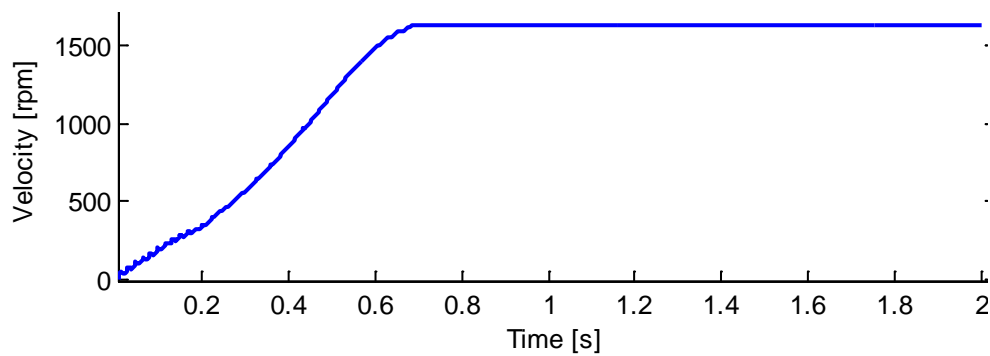


Figure 32: Rotor frequency



**Figure 33:** Electromagnetic torque of the induction machine



**Figure 34:** Velocity of the induction machine

Considering that the induction machine is fed from the stator with a harmonic voltage source  $V_{sh}$  with frequency  $f_{sh}$  and in the rotor a harmonic voltage source  $V_{rh}$  with frequency  $f_{rh}$ . The voltage source is 460 V at 60 Hz in the stator, which includes the third, fifth, and seventh harmonics. The voltage source in rotor is 50 V at 45 Hz, which includes the third, fifth, and seventh harmonics. The magnitudes and angles of the components of the harmonic voltages are shown in Table 4.

**Table 4:** Harmonic components of the stator and rotor voltage

STATOR				
	Fundamental	Third	Fifth	Seventh
<b>Magnitude</b>	460	153.3	92	65.714
<b>Angle</b>	30°	113°	42.85°	137.15°
ROTOR				
	Fundamental	Third	Fifth	Seventh
<b>Magnitude</b>	50	16.7	10	7.142
<b>Angle</b>	13.6°	8.63°	114.5°	47.32°

The stator and rotor currents modeled in both states are shown in **Figure 35** and **Figure 37**, respectively. A mechanical torque of 198 N × m is also used for this case study.

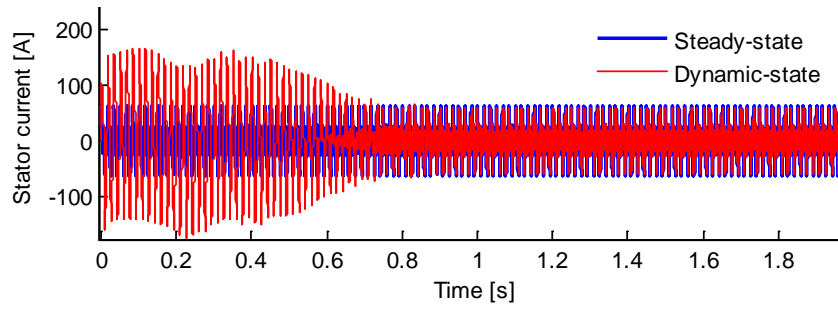


**Figure 35:** Stator current

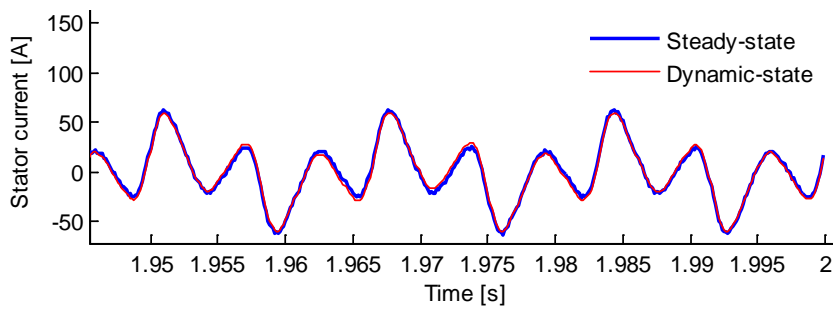


**Figure 36:** Zoom of the Figure 35

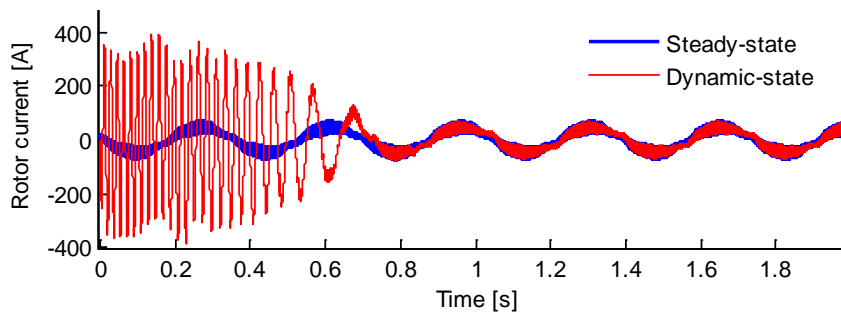


**Figure 37:** Rotor current

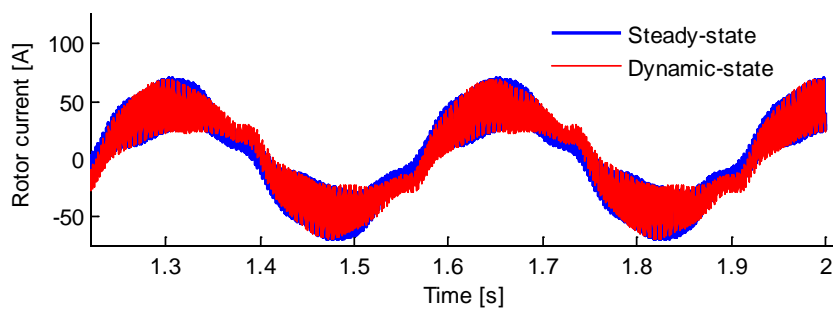


**Figure 38:** Zoom of the Figure 37

Considering a slip value of 0.96, the fundamental frequency that the stator winding induces the rotor winding, according to (16),

$$\frac{s_h \times h \times \omega_{es}}{2\pi} = \frac{0.96 \times 1 \times 377}{2\pi} = 57.60 \text{ Hz}$$

The fifth harmonic inducing the stator winding to the rotor winding will be

$$\frac{s_5 \times h \times \omega_{es}}{2\pi} = \frac{1.15 \times 5 \times 377}{2\pi} = 345.18 \text{ Hz}$$

Finally, the seventh harmonic, inducing the stator winding to the rotor winding, will be

$$\frac{s_7 \times h \times \omega_{es}}{2\pi} = \frac{0.86 \times 7 \times 377}{2\pi} = 361.4 \text{ Hz}$$

These frequencies can be observed in **Figure 39** and **Figure 40** in which are shown the induced frequencies of the stator to the rotor, respectively, in according with the previous analysis.

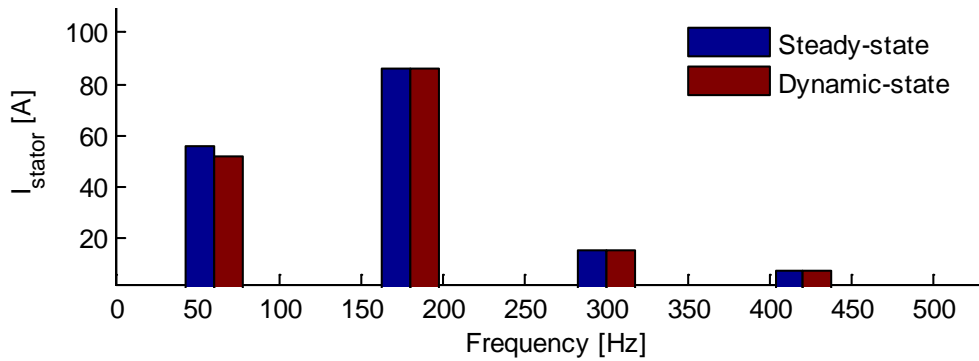


**Figure 39:** Stator frequencies

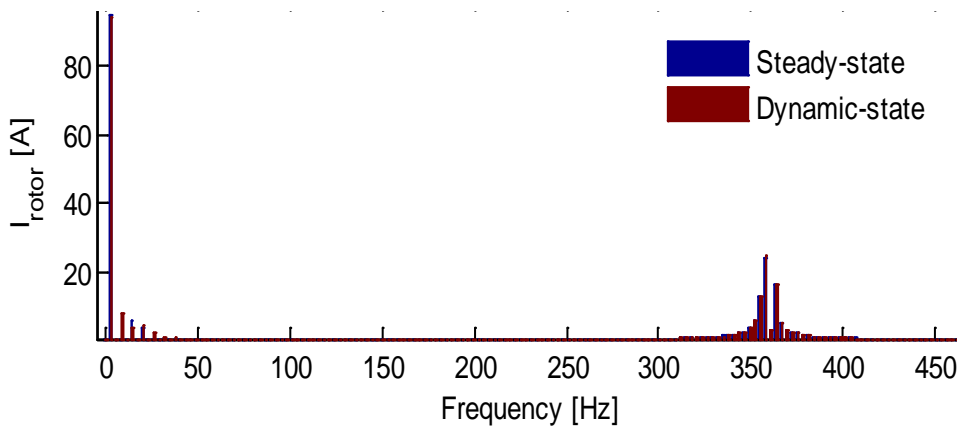


**Figure 40:** Rotor frequencies

Table V summarizes the harmonic currents in the induction machine for the case studies. Note that the waveform current presented in the paper has been attained from current shown in this table, which have been obtained from the solution of the equations mentioned in the previous section.

**Table 5:** Summary of the harmonic currents for this case study

STATOR				ROTOR			
Sequence	Magnitude	Angle	Frequency	Sequence	Magnitude	Angle	Frequency
+	460	180.6°	60 Hz	+	45	204.9°	45 Hz
0	153.3	183.2°	180 Hz	0	15	-78.3°	193.5 Hz
-	260	181.2°	300 Hz	-	9	-85.1°	607.8 Hz
+	71.42	179.2°	420 Hz	+	6.42	-28.4°	1122 Hz
-	41.81	18.2°	610.2 Hz	-	2.65	120.2°	457.65 Hz
+	35.38	-5.8°	267 Hz	+	2.36	117°	200.25 Hz

#### 4. Conclusion

This research proposed a steady-state model for the squirrel cage induction machine and doubly-fed induction machine for harmonic and inter-harmonic studies. The currents response of the different wind energy conversion system are obtained of the mathematical model when it is fed with sinusoidal and nonsinusoidal voltage sources. Depending on the slip and the fundamental frequency of both voltage sources the current harmonics and non-harmonics can exist on both sides of the machine. The simulation results obtained with the steady-state proposed model were compared with those obtained from dynamic simulation, where the comparison between them is in complete agreement. Finally, this research gives a clear analysis of the frequencies generated by the wind energy conversion system, in steady-state, resulting in a clear and precise model for harmonic and inter-harmonic analysis, which can be used for “harmonic” analysis in a power system.

#### References

- [1] T. Ackermann. “Wind power in power systems”, Wiley, 2005.
- [2] J. Martínez García, M. García-García, M. P. Comech, D. García-García, “Modelling and simulation of an asynchronous wind turbine of squirrel cage”, ICREPQ’04 Proceeding, 31 March – 02 April 2004, Barcelona.
- [3] J. G. Slootweg, W. L. Kling, “Is the answer blowing in the wind?” IEEE Power & Energy Magazine, pp 26-33, Nov/Dec 2003.
- [4] R. Datta, V. T. Ranganathan, “Variable-speed wind power generation using doubly-fed wind rotor induction machine a comparison with alternative schmes.”, IEEE Transactions on Energy Conversion, vol. 17, no. 3, p.p. 414-421, Sept. 2002.
- [5] P. C. Krause, Analysis of Electric Machinery. New York, NY, USA: McGraw-Hill, 1987.
- [6] E. H. Camm, M. R. Behnke, O. Bolado, M. Bollen, M. Bradt, C. Brooks, W. Dilling, M. Edds, W. J. Hejidak, D. Houseman, S. Klien, F. Li, J. Li, P. Maibach, T. Nicolai, J. Patino, S. V. Pasupulati, N. Samaan, S. Saylors, T. Seibert, T. Smith, M. Starke, and R. Walling, “Wind power plant grounding, overvoltage protection and insulation coordination: IEEE PES Wind Plant Collector System Design

- Working Group,” in Proc. IEEE Power and Energy Soc. General Meet., 2009, pp. 1–8.
- [7] L. Fan, S. Yuvurajan and R. Kavasseri, “Harmonic Analysis of a DFIG for a Wind Energy Conversion System” IEEE Trans. Energy Convers., vol. 25, no. 1, pp. 181-190, March. 2010.
- [8] A. Tapia, G. Tapia, J.S. Ostolaza, J.R. Saenz, .“Modeling and control of a wind turbine driven doubly fed induction generator.”, IEEE Transactions on Energy Conversion, vol. 18, no. 2, pp. 194-204, June 2003.
- [9] J. Morren, S.W.H. Haan, .“Ride through of wind turbines with doubly fed induction generator during a voltage dip.”, IEEE Transactions on Energy Conversion, vol. 20, no. 2, pp. 435-441, June 2005.
- [10] I. Erlich, W. Winter, A. Dittrich, “Advanced Grid Requirements for the Integration of Wind Turbines into the German transmission system.”, 2006 IEEE Power Engineering Society General Meeting, 18-22 June 2006, pp. 7.
- [11] Peña R., Clare J.C. y Ascher G.M., “Doubly Fed Induction Generator using back to back PWM converters and its application to variable-speed wind energy generation”, IEE Proceeding Electric Power Applications, Vol. 43, No. 3, pp. 231-241, Mar 1996.
- [12] Müller S., Deicke M. y De Doncker R., “Doubly Fed Induction Generator Systems for Wind Turbines”, IEEE Industry Applications Magazine, pp. 26-33, May-June 2002.
- [13] Kundur Prabha, Power System Stability and Control. New York: McGraw-Hill, 1994.
- [14] Krause Paul, Wasynczuk Oleg and Sudhoff Scott, Analysis of Electric Machinery. New York: IEEE Press, 1995